JOURNAL OF COMPUTATIONAL PHYSICS 21, 333–339 (1976)

Note

A Boundary Condition for Significantly Reducing Boundary Reflections with a Lagrangian Mesh*

INTRODUCTION

Reflections from the terminating mesh boundaries are an important consideration in the selection of the calculational grid size for the numerical solution of hyperbolic equations. The rationale for selecting the calculational grid is complicated by several factors. On one hand we desire both a fine grid to optimize resolution, and boundaries far from the region of interest to minimize or delay unphysical reflections. On the other hand economic limitations, such as available memory or computer time, permit only coarse grids and nearby boundaries.

Obviously, terminating boundary conditions that eliminate boundary reflections or significantly reduce their amplitude are desirable. Some techniques have been applied for this purpose. For example, a boundary description thought to scatter the impinging waves has been applied with some two-dimensional Lagrangian codes. This technique calculates the velocities on alternate boundary nodes while setting the velocities on the other set of boundary nodes to zero for a given time-step. The roles are reversed in the next calculational time-step and this procedure continues. This technique has been applied in the TENSOR two-dimensional Lagrangian code [1]. A search of the literature has not revealed information discussing characteristics of the scattering technique.

An adjusted damper system along the boundaries is another technique for significantly reducing the boundary reflections and is the subject of this paper. Although the method is analyzed below in one dimension, it has been applied in a TEMS two-dimensional plane calculation [2]. The results are compared with those in which the scattering technique was applied along the boundary, also in a TEMS calculation.

* Notice: This report was prepared as an account of work sponsored by the United States Government. Neither the United States nor the United States Energy Research & Development Administration, nor any of their employees, nor any of their contractors, subcontractors, or their employees, makes any warranty, express or implied, or assumes any legal liability or responsibility for the accuracy, completeness or usefulness of any information, apparatus, product or process disclosed, or represents that its use would not infringe privately owned rights.

THEORY

A spring-dashpot system used as the terminating network on a one-dimensional elastic system can be designed to absorb a single wavelength with the appropriate choice of parameters. In the limit as the spring constant of the terminating spring approaches zero, the reflection coefficient predicted by a one-dimensional analysis is minimized over a range of wavelengths of interest. Hence the description of the network terminated with only the dashpot is applied. The governing equations describing this system are well known. If we apply the following Fourier expansion to these equations

$$X_j = \exp(-i(j/\bar{\lambda} + \omega t)) + R\exp(+i(j/\bar{\lambda} - \omega t)), \tag{1}$$

where $\bar{\lambda}$ is the reduced wavelength (that is $\bar{\lambda} = \lambda/2\pi\Delta X$), the form of the reflection coefficient R is found to be

$$R = \frac{\Lambda(1 - (2m_0/m)) + i((1 - \Lambda^2)^{1/2} - (C/(mK)^{1/2}))}{\Lambda(-1 + (2m_0/m)) + i((1 - \Lambda^2)^{1/2} + (C/(mK)^{1/2}))}, \tag{2}$$

where $\Lambda = \sin 1/(2\bar{\lambda})$, $\omega = 2(K/m)^{1/2}(\sin 1/(2\bar{\lambda}))$, K is the spring constant within the mesh, C is the coefficient of daming of the terminating dashpot, m is the nodal mass within the mesh, and m_0 is the terminating mass.

Normally with fairly uniform calculational meshes in one and more spatial dimensions, the terminating boundary mass m_0 is about half the interior masses. For $m_0 = m/2$, the reflection coefficient becomes

$$R = \frac{(1 - \Lambda^2)^{1/2} - C/(mK)^{1/2}}{(1 - \Lambda^2)^{1/2} + C/(mK)^{1/2}} = \frac{\cos 1/(2\bar{\lambda}) - \cos 1/(2\bar{\lambda}_0)}{\cos 1/(2\bar{\lambda}) + \cos 1/(2\bar{\lambda}_0)}, \tag{3}$$

where $\bar{\lambda}_0$ is the reduced wavelength at the position of no reflection. Figure 1 displays the reflection characteristics for $\xi_0 = 5$ and $\xi_0 = 10$ (for $3 < \xi < 25$, $\xi_0 = 2\pi\bar{\lambda}_0$, the wavelength in zone units).

When the terminating mass is not equal to half of an internal mesh mass the form of the reflection coefficient is more complicated. Ignoring the phase angle, the magnitude of the reflection coefficient is

$$|R| = \left\{\frac{(1 - (2m_0/m))^2 \sin^2 1/(2\bar{\lambda}) + [\cos 1/(2\bar{\lambda}) - \cos 1/(2\bar{\lambda}_0)]^2}{(1 - (2m_0/m))^2 \sin^2 1/(2\bar{\lambda}) + [\cos 1/(2\bar{\lambda}) + \cos 1/(2\bar{\lambda}_0)]^2}\right\}^{1/2}, \tag{4}$$

where $\bar{\lambda}_0$ is defined in Eq. (3). As an example of what effect this has on the reflection characteristics, Fig. 2 shows the amplitude of the reflection, $|R|$, for $m_0 = m$ and $m_0 = 7/16m$ or $9/16m$, both with $\xi_0 = 5$.

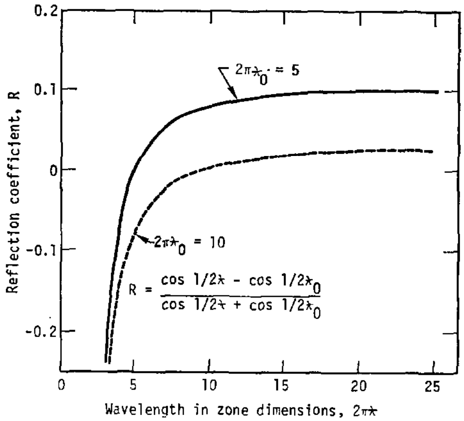

FIG. 1. Reflection coefficient as a function of wavelength in zone dimensions for the parameters shown.

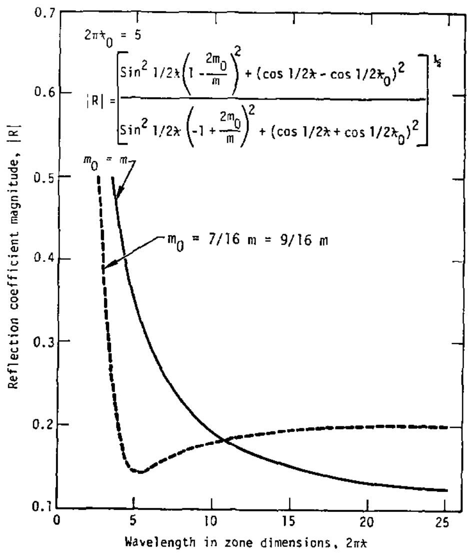

FIG. 2. Magnitude of the reflection coefficient as a function of wavelength in zone dimensions for the parameters shown.

RESULTS

The TEMS [2] two-dimensional, elastic, dynamic code was used to compare the following boundary termination conditions: a fixed boundary, a scattering boundary, and the damping condition, which is the subject of this paper. A 30×60 mesh was applied with the elastic material having a density of $2.7\ \mathrm{Mg/m^3}$, a Young's modulus, $E = 2.5 \times 10^{10}$ Pa, and a Poisson's ratio of 0.25 implying a compressional wave speed of $3.33\ \mathrm{mm}/\mu\mathrm{sec}$. The zones in the calculation were square and, except for the corners, the boundary masses were half the internal masses. The calculations were performed in plane strain.

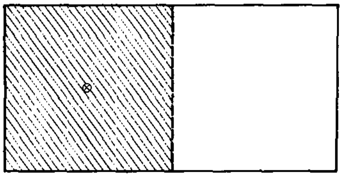

FIG. 3. Geometry of the two-dimensional calculations.

A circular source was applied at the center of one end of the mesh, at equal distance from both sides and one end (Fig. 3). The appropriate boundary condition was applied along the entire periphery of the mesh to both the tangnetial and normal components of velocity. For the damping boundary, the damping coefficient is given by

$$C = (Km/V)^{1/2} \cos 1/(2\lambda_0), \tag{5}$$

where λ_0 is defined in Eq. (3), m is mass of the point just internal to the boundary, K is a combination of the Lame constants of a zone adjacent to the boundary mass, and V is the volume of the adjacent zone. For the velocity component perpendicular to the boundary,

$$K = E(1 - \nu)/[(1 + \nu)(1 - 2\nu)]$$

in Eq. (5), while $E/2(1 + \nu)$ was used for K to damp the velocity component parallel to the boundary.

A sinusoidally varying pressure with a wavelength of seven zones was applied as the source, and the calculations were continued until the waves generated by this source impinged on the boundaries. The source characteristics remained unchanged in the calculations for each variation in the boundary condition (fixed, scattering, and damping).

To assess the effects of the boundaries on the impinging waves, the first invariant of the strain tensor (dilatation) adjacent to the boundary was compared to the dilatation along a gemetrically similar line in the free field, taken to be the bisector of the long axis of the grid (Fig. 3).

Comparison was made by subtracting the values of the dilatation along a line through the free field from the value of this parameter just inside the boundary. The position of these lines is chosen to be geometrically similar with respect to the source. Figure 4 shows the results of subtracting the free-field dilatation from that along the boundary for the damping, scattering, and fixed boundaries. These dilatation plots are shown for the time at which the magnitude of the dilatation from the first impinging wave was largest. This time was 1.57 T', where T' is the compressional wave traversal time from the sources to the near boundaries.

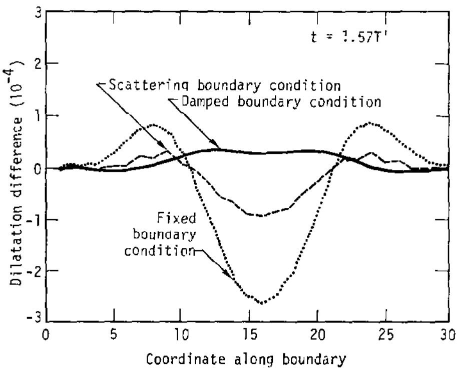

FIG. 4. Dilatation difference as a function of the coordinate along boundary for the damped, scattering, and fixed boundary conditions.

DISCUSSION AND CONCLUSIONS

The phase of the dilatation just inside the boundary is similar for the damping, scattering, and fixed boundary conditions (Fig. 4).

The subtraction of the values along a line in the free field from those along the boundary provides a quantitive comparison. For example, if the maximum magnitude of the dilatation difference (the maximum magnitude being defined as the difference between the maximum and the minimum on the plot) for the case with the damped boundary condition is compared with the fixed case, we note that this magnitude is about 11 % of the value for the free case. Comparing these numbers with the case having the scattering boundary, we note that the difference is about 35 % of the value for the fixed case. Hence, with this parameter as a measure, the damping boundary reflects less than 33 % as much as the scattering boundary.

The parameter ξ_0 (minimum reflection wavelength) was chosen as five zones for these calculations. The magnitude of the reflection coefficient is bounded by 0.1 over a reasonable range of frequencies (Fig. 1 for $2\pi\lambda_0 = 5$). The minimum wavelength passed by a Lagrangian mesh is 2 zones; however, the calculations will be extremely dispersive at this wavelength. Also, the group velocity is zero at the wavelength of two zones, hence the short wavelength reflections will be delayed. Experience with the technique has shown that nonlinearities such as fractures near or through the boundary can result in severe instabilities.

The fraction of boundary reflection with the damping condition as compared to the fixed (Fig. 4) boundary, is somewhat larger than that predicted for a wavelength of seven zones (Fig. 1). This can be explained by the fact that the analysis of the technique was performed in one dimension and the technique was applied in two dimensions.

Some additional analyses were performed to check the characteristics of the spring constant on the tangential component. These calculations showed that the magnitude of the reflection was greater when the constant K (Eq. 5) for the tangential component, was taken to be $E(1 - \nu)/[(1 + \nu)(1 - 2\nu)]$ instead of $E/2(1 + \nu)$. A similar result was obtained when the tangential spring constant was set to zero.

For applications, the boundaries should be placed somewhat away from the region of interest. Some calculations have been performed with these damping boundaries as close as 5 or 10 zones from regions of interest and little effect of the boundaries could be seen. On another occassion, these boundary conditions have been used to simulate the coupling along a real physical boundary. In that case, some tuning of the coefficients was required. These conditions have been applied only for plane geometries; they have not been tested for cylindrical or spherical geometries.

In conclusion, the damping condition developed here results in reflections that are about 11 % of the amplitude of the reflection from a fixed or free boundary, and about 33 % of that from a scattering boundary used to reduce the terminating boundary effects.

Acknowledgment

This work was in part performed under the auspices of the U. S. Energy Research & Development Administration, under contract No. W-7405-Eng-48.

References

1. G. Maenchen and S. Sack, *in* "Methods in Computational Physics," Vol. 3 (B. Alder, Ed.), Academic Press, New York, 1964.
2. A. G. Petschek and M. E. Hanson, *J. Comput. Phys.* **3** (1968), 307–321.

Received: June 24, 1975; revised: December 1, 1975

M. E. Hanson

Laurence Livermore Laboratory,
University of California,
P.O. Box 808,
Livermore, California 94550

A. G. Petschek

New Mexico Institute of Mining and Technology
Campus Station,
Socorro, New Mexico 87801